Inorganic Chemistry

ARTICLE

pubs.acs.org/IC

Tetra-2,3-pyrazinoporphyrazines with Externally Appended Thienyl Rings: Synthesis, UV−Visible Spectra, Electrochemical Behavior, and Photoactivity for the Generation of Singlet Oxygen

Giorgia De Mori,[†] Zhen Fu,[‡] Elisa Viola,[†] Xiaohui Cai,[‡] Claudio Ercolani,[†] Maria Pia Donzello,*[,†] and Karl M. Kadish*[,‡]

[†]Dipartimento di Chimica, Università di Roma "La Sapienza", P.le A. Moro 5, I-00185 Roma, Italy

[‡]Department of Chemistry, University of Houston, Houston, Texas 77204-5003, United States

Supporting Information

ABSTRACT: A series of pyrazinoporphyrazine macrocycles carrying externally appended 2-thienyl rings, represented as [Th_8TPyzPzM], where Th_8TPyzPz = tetrakis-2,3-[5,6-di(2-thienyl)pyrazino]porphyrazinato anion and M = $Mg^{II}(H_2O)$, Zn^{II}, Co^{II}, Cu^{II}, or $2H^1$, were prepared and isolated as solid air-stable hydrated species. All of the compounds, completely insoluble in water, were characterized by their UV−visible spectra and electrochemical behavior in solutions of dimethylformamide (DMF), dimethyl sulfoxide, and pyridine. Molecular aggregation occurs at concentrations of ca. 10^{-4} M, but monomers are formed in more dilute solutions of 10^{-5} M or less. The examined octathienyl compounds [Th_8TPyzPzM] behave as electron-deficient macrocycles, and UV−visible spectral measurements provide useful information about how the peripheral thienyl rings influence the electronic distribution over the entire macrocyclic framework. Cyclic voltammetric and spectroelectrochemical data confirm the easier reducibility of the compounds as compared to the related phthalocyanine analogues, and the overall redox behavior and thermodynamic potentials for the four stepwise one-electron reductions of the compounds are similar to those of the earlier examined octapyridinated analogues [Py_8TPyzPzM]. Quantum yields (Φ_Δ) for the generation of singlet oxygen, $^1O_2$, the cytotoxic agent active in photodynamic therapy (PDT), and fluorescence quantum yields (Φ_F) were measured for the Zn^{II} and Mg^{II} complexes, [Th_8TPyzPzZn] and [Th_8TPyzPzMg(H_2O)], and the data were compared to those of corresponding octapyridino macrocycles [Py_8TPyzPzZn] and [Py_8TPyzPzMg(H_2O)] and their related octacations [(2-Mepy)$_8$TPyzPzZn]$^{8+}$ and [(2-Mepy)$_8$TPyzPzMg(H_2O)]$^{8+}$. These measurements were carried out in DMF and in DMF preacidified with HCl (ca. 10^{-4} M). All of the examined Zn^{II} compounds behave as excellent photosensitizers (Φ_Δ = 0.4−0.6) both in DMF and DMF/HCl solutions, whereas noticeable fluorescence activity (Φ_F = 0.36−0.43) in DMF/HCl solutions is shown by the Mg^{II} derivatives; these data might provide perspectives for applications in PDT (Zn^{II}) and imaging response and diagnosis (Mg^{II}).

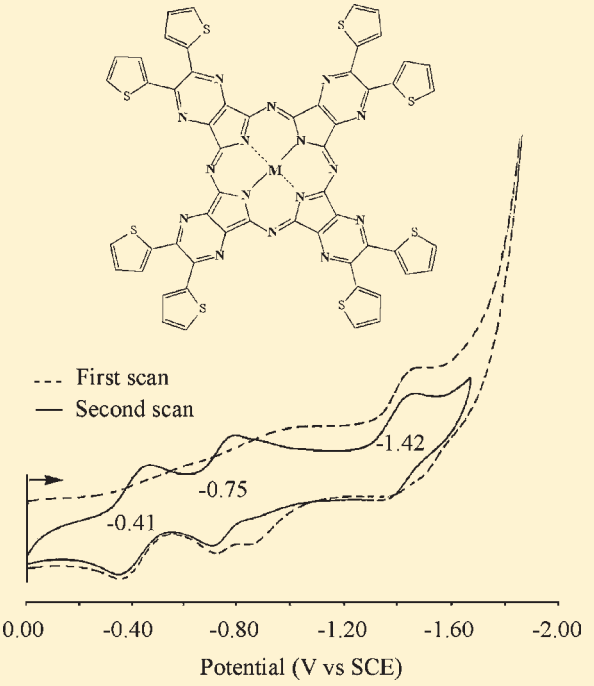

INTRODUCTION

Porphyrazines, apart from the phthalocyanine family (tetrabenzoporphyrazines), have received increasing attention over the past decade.[1] Our own group has concentrated, in part, on the synthesis and characterization of (thia/seleno)diazolporphyrazines,[2] diazepinoporphyrazines,[3] and pyrazinoporphyrazines,[4,5] the latter of which are represented by [Py_8TPyzPzM] where Py_8TPyzPz = tetrakis-2,3-[5,6-di(2-pyridyl)pyrazino]porphyrazinato anion and M = $Mg^{II}(H_2O)$, Mn^{II}, Co^{II}, Cu^{II}, Zn^{II}, Pd^{II}, or $2H^1$. All of the studied porphyrazines can be characterized as electron-deficient macrocycles on the basis of their UV−visible spectral features and electrochemical behavior, and in the case of pyrazinoporphyrazines (Chart 1A), the exocyclic pendant vicinal pyridine rings will strongly influence the electronic structure of the macrocycle, so much so that the compounds become remarkably easier to reduce than their related phthalocyanine analogues.[4−6] In nonaqueous media, the electrochemical processes occur via

Received: April 12, 2011
Published: July 27, 2011

Chart 1. Schematic Representation of the Macrocycles [Py_8TPyzPzM] (A) and [Th_8TPyzPzM] (B) [M = $Mg^{II}(H_2O)$, Zn^{II}, Cu^{II}, Co^{II}, and $2H^{I}$]

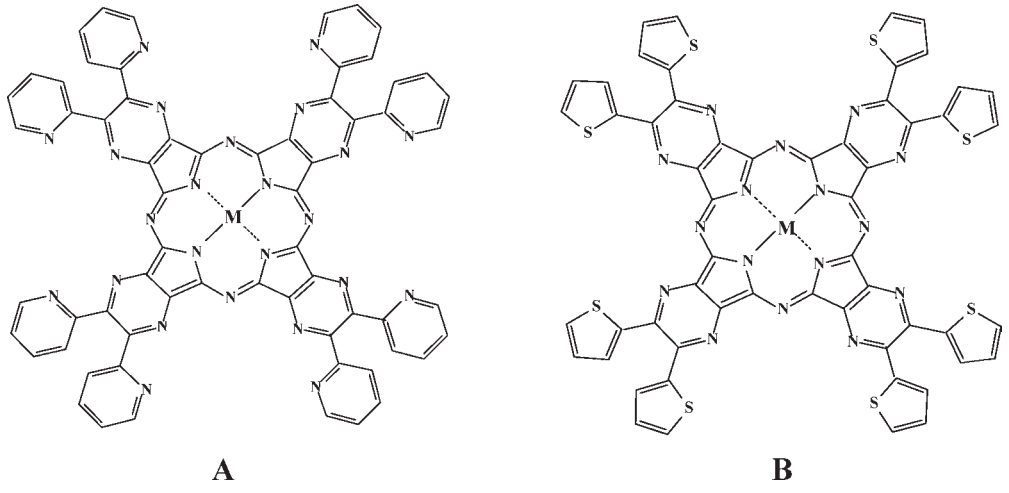

stepwise one-electron additions to give stable species with charges of 1−, 2−, 3−, and 4−. Quaternization of N atoms in the pyridine rings leads to the formation of a parallel series of water-soluble octacationic macrocycles, $[(2\text{-Mepy})_8\text{TPyzPzM}]^{8+}$ (neutralized by I^- ions; Figure S1A in the Supporting Information),[5,6] while coordination of $PdCl_2$ on the same pyridine rings ("py−py" coordination) results in the formation of related homo- and heteropentametallic macrocycles, $[(PdCl_2)_4Py_8\text{TPyzPzPd}]$[5] and $[(PdCl_2)_4Py_8\text{TPyzPzM}]$,[7] where M = Zn^{II}, Cu^{II}, $Mg^{II}(H_2O)$, or Cd^{II} (Figure S1B in the Supporting Information). The electron deficiency of the entire macrocyclic unit upon quaternization or exocyclic coordination of Pd^{II} results in easier reductions, and this change in the electron density is also seen in UV−visible spectra of the +8 charged or neutral externally palladated compounds, which exhibit 5−15 nm bathochromic shifts of the Q band with respect to the related starting monometallic species.

In light of the above data for externally pyridinated pyrazinoporphyrazines, we have extended our studies to include a related series of compounds carrying external thienyl rings. These porphyrazines have the formula [Th_8TPyzPzM], where Th_8TPyzPz = tetrakis-2,3-[5,6-di(2-thienyl)pyrazino]porphyrazinato anion and M = $Mg^{II}(H_2O)$, Zn^{II}, Cu^{II}, Co^{II}, or $2H^{I}$ (Chart 1B). The role played by the external thienyl rings in the electronic distribution within the entire molecular framework of the title macrocycles is the target of the present study, mainly conducted by UV−visible spectral and electrochemical investigation in solution of low-donor solvents.

Porphyrins and phthalocyanines are of central importance for their use as photosensitizers in photodynamic therapy (PDT), presently one of the most widely studied therapeutic modalities of cancer or noncancerous tissue illnesses.[8] PDT implies the use of a photosensitizer, light, and dioxygen ($^3O_2$). Singlet oxygen, $^1O_2$, the active anticancer agent, can be generated from $^3O_2$ in the process $^3O_2 \rightarrow {}^1O_2$ by energy transfer to $^3O_2$ from a photoexcited sensitizer irradiated with light of an appropriate wavelength (600−800 nm). Although excellent photoactivity for the formation of singlet oxygen in nonaqueous media has been demonstrated for a variety of substituted tetrapyrazinoporphyrazines,[9] secoporphyrazines,[10] and benzonaphthoporphyrazines,[11] more extended information is needed on the role of porphyrazines in the field of PDT. This is also addressed in the current work where quantum yields for singlet oxygen production (Φ_Δ) and the fluorescence response (Φ_F) measured are reported for the complexes [Th_8TPyzPzM] [M = Zn^{II} and $Mg^{II}(H_2O)$] and related macrocycles in dimethylformamide (DMF) and DMF preacidified with HCl (DMF/HCl).

EXPERIMENTAL SECTION

Solvents and chemicals were used as purchased, unless specified otherwise. The synthesis of 2,3-dicyano-5,6-di(2-thienyl)pyrazine, $[(CN)_2\text{-}Th_2Pyz]$, from 2,2′-thienyl and diaminomaleonitrile was as previously reported.[12] In our procedure, variations were made for extraction and purification of the compound. Details of the synthesis are as follows: 2,2′-thienyl (890 mg, 3.99 mmol) and diaminomaleonitrile (569 mg, 4.99 mmol) (molar ratio 4:5) were added to CH_3COOH (20 mL) in a 50 mL flask, and the mixture was heated to 140 °C and stirred for 16 h. After cooling and separation of any solid present, the solvent was evaporated and the solid obtained was washed repeatedly with warm water and brought to a constant weight under vacuum. After Soxhlet extraction of the solid with dichloromethane followed by evaporation of the solvent, the solid residue was first brought to a constant weight under vacuum and then purified by crystallization from chloroform (30 mL) and hexane (20 mL). The yellow-orange needle crystals melt at 178−180 °C (610 mg; yield 52%). Calcd for $C_{14}H_6N_4S_2$: C, 57.13; H, 2.05; N, 19.03; S, 21.79. Found: C, 56.94; H, 2.01; N, 18.70; S, 20.91%. IR (KBr, cm^{-1}): 3100 (CH, w), 2240 (CN, vw), 1747 (w), 1537 (w), 1508 (m), 1499 (m), 1440 (w), 1418 (s), 1385 (vvs), 1331 (vvw), 1313 (vvw), 1273 (w), 1230 (w), 1221 (vw), 1190 (w), 1121 (vw), 1076 (w), 1059 (w-m), 987 (vw), 883 (vw), 854 (m), 845 (m), 738 (m), 727 (s), 692 (vw), 659 (vw) 575 (w-m), 517 (w-m), 345 (m).

Synthesis of [Th_8TPyzPzMg(H_2O)]·$3H_2O$. The synthesis of this compound from magnesium(II) butoxide and 2,3-dicyano-5,6-di(2-thienyl)pyrazine, $[(CN)_2Th_2Pyz]$, has been reported in two previous papers.[12,13] In the present study, the following modified synthetic procedure was used: magnesium (90 mg, 3.7 mmol), propyl alcohol (15 mL), and a few crystals of iodine were mixed in a small flask (25 mL) and the mixture was heated to reflux under stirring for 16 h. The dicyano precursor $[(CN)_2Th_2Pyz]$ (300 mg) was then added and the mixture refluxed for 8 more hours, after which it was brought to room temperature and poured into a vessel and the solvent left to evaporate completely. To the solid residue was added 50% CH_3COOH (10 mL) and the mixture kept under stirring for 1 h, after which the solid was

dx.doi.org/10.1021/ic2007556 |Inorg. Chem. 2011, 50, 8225–8237

separated by centrifugation, washed repeatedly with ether and then with acetone, and finally brought to a constant weight under vacuum (10^{-2} mmHg; 270 mg; yield 83%). Calcd for $[Th_8TPyzPzMg(H_2O)]\cdot 3H_2O$, $C_{56}H_{32}MgN_{16}O_3S_8$: C, 52.81; H, 2.53; N, 17.59; S, 20.14. Found: C, 52.59; H, 2.23; N, 16.79; S, 20.29%. The water content for this compound was not constant and varied slightly with each batch prepared. IR (KBr, cm^{-1}): 3400 (broad), 1634 (w), 1516 (w), 1481 (vw), 1421 (vw), 1362 (w), 1312 (m), 1254 (w), 1231 (m), 1170 (m), 1084 (w-m), 905 (m-s), 851 (m), 777 (m-s), 747 (m), 703 (s), 524 (w).

Synthesis of $[Th_8TPyzPzH_2]\cdot CF_3COOH\cdot H_2O$. The free-base macrocycle was prepared as follows: the Mg^{II} complex $[Th_8TPyzPzMg(H_2O)]\cdot 3H_2O$ (200 mg, 0.157 mmol) was suspended, partly dissolved, in CF_3COOH (4 mL) and the mixture refluxed under stirring for 5 h. After cooling, water was added to the mixture (cautiously!) and the bluish-black solid was separated by centrifugation, washed several times with water until neutrality of the mother liquors and then with acetone, and finally brought to a constant weight under vacuum (10^{-2} mmHg; 155 mg; yield 77%). Calcd for $[Th_8TPyzPzH_2]\cdot CF_3COOH\cdot H_2O$, $C_{56}H_{26}N_{16}S_8(CF_3COOH)(H_2O)$: C, 53.12; H, 2.23; N, 17.09; S, 19.56. Found: C, 53.52; H, 2.54; N, 16.93; S, 19.64%. IR (KBr, cm^{-1}): 3400 (broad), 3300 (w, ν_{N-H}), 1736 (w-m), 1518 (m), 1423 (m), 1385 (vs), 1319 (vs), 1309 (w) (sh), 1230 (w), 1202 (w), 1175 (vw), 1136 (m-s), 1084 (w), 1022 (vw), 904 (w), 852 (m), 841 (m), 777 (w), 744 (m), 708 (s), 690 (w), 523 (w).

Synthesis of $[Th_8TPyzPzZn]\cdot 4H_2O$. A previously reported synthesis of $[Th_8TPyzPzZn]\cdot 4H_2O$[13] was modified according to the following procedure: $[Th_8TPyzPzH_2]\cdot CF_3COOH\cdot H_2O$ (61 mg, 0.047 mmol) and $Zn(OAc)_2\cdot 2H_2O$ (56 mg, 0.25 mmol) (molar ratio 1:5) were suspended in freshly distilled dimethyl sulfoxide (DMSO; 3 mL), and the mixture was then heated to 120 °C and kept at this temperature while stirring for 6 h. After cooling and centrifugation, the separated dark-green solid was washed repeatedly with water and acetone and brought to a constant weight under vacuum (10^{-2} mmHg; 47 mg; yield 62%). Calcd for $[Th_8TPyzPzZn]\cdot 4H_2O$, $C_{56}H_{32}N_{16}O_4S_8Zn$: C, 51.14; H, 2.45; N, 17.04; S, 19.51. Found: C, 50.87; H, 1.99; N, 16.70; S, 20.02%. IR (KBr, cm^{-1}): 3400 (broad), 1628 (w), 1543 (vw), 1514 (w-m), 1485 (w),1455 (w), 1421 (m-s), 1362 (m), 1322 (m), 1317 (m), 1250 (m), 1232 (m), 1180 (m), 1101 (m-s), 1049 (w), 996 (vw), 951 (w), 904 (m-s), 854 (m), 812 (vw), 774 (m-s), 746 (m), 700 (s), 666 (w), 634 (w), 566 (w), 523 (w), 452 (w).

Synthesis of $[Th_8TPyzPzCu]\cdot 4H_2O$. The Cu^{II} complex was prepared using a procedure similar to that reported above for the Zn^{II} derivative. The same product was obtained in pyridine or DMSO, and the synthesis in DMSO was carried out as follows: $[Th_8TPyzPzH_2]\cdot CF_3COOH\cdot H_2O$ (35 mg, 0.027 mmol) and $Cu(OAc)_2\cdot H_2O$ (27.5 mg, 0.151 mmol) (molar ratio 1:5) were suspended in freshly distilled DMSO, and the mixture was heated to 120 °C while stirring for 6 h. After cooling and filtration, the separated dark-green solid was washed repeatedly with water and acetone and then brought to a constant weight under vacuum (10^{-2} mmHg; 21 mg; yield 55%). Calcd for $[Th_8TPyzPzCu]\cdot 4H_2O$, $C_{56}H_{32}CuN_{16}O_4S_8$: C, 51.23; H, 2.46; N, 17.07; S, 19.53. Found: C, 51.53; H, 1.98; N, 16.62; S, 18.02%. IR (KBr, cm^{-1}): 3400 (broad), 1628 (vw), 1549 (vw), 1516 (w-m), 1471 (w), 1421 (s), 1362 (s), 1316 (m), 1255 (w), 1232 (w-m), 1186 (w), 1109 (m), 1087 (vw), 1060 (vw), 912 (m), 854 (w), 825 (w), 809 (vw), 778 (m), 748 (w), 703 (s), 520 (w).

Synthesis of $[Th_8TPyzPzCo]\cdot 7H_2O$. $[Th_8TPyzPzH_2]\cdot CF_3COOH\cdot H_2O$ (30.8 mg, 0.024 mmol) and $Co(OAc)_2\cdot 4H_2O$ (34.1 mg, 0.136 mmol) (molar ratio 1:5) were suspended in freshly distilled DMSO (3 mL), after which the mixture was heated to 120 °C and stirred for 6 h. After cooling and centrifugation, the separated dark-green solid was washed repeatedly with water and then with acetone and brought to a constant weight under vacuum (10^{-2} mmHg; 17 mg; yield 50.4%). Calcd for $[Th_8TPyzPzCo]\cdot 7H_2O$, $C_{56}H_{38}CoN_{16}O_7S_8$: C, 49.37; H, 2.81, N, 16.45, S, 18.83. Found: C, 49.37; H, 2.18; N, 15.97, S, 17.49%. IR (KBr, cm^{-1}): 3400 (broad), 1628 (w), 1556 (w), 1520 (w-m), 1479 (w), 1421 (s), 1361 (s), 1317 (s), 1256 (w-m), 1231 (m), 1174 (m), 1114 (s), 1084 (w), 1060 (w), 922 (m), 904 (w), 853 (m), 809 (vw), 779 (s), 752 (w), 747 (w), 706 (vs), 665 (w), 570 (w), 525 (w), 455 (vw).

Electrochemical and Spectroelectrochemical Measurements. The solvents used for electrochemical measurements, pyridine (99.9+%), DMSO (99.9+%), and DMF (99.8+%), were purchased from Sigma-Aldrich Co. and used without further purification. High-purity N_2 from Trigas was used to deoxygenate the solution before each electrochemical and spectroelectrochemical experiment. Tetra-*n*-butylammonium perchlorate (TBAP; 99%) from Fluka Chemika Co. was used as a supporting electrolyte (0.1 M for cyclic voltammetry and 0.2 M for spectroelectrochemistry) and stored under vacuum at 40 °C prior to use.

Cyclic voltammetry was performed with an EG&G model 173 potentiostat coupled to an EG&G model 175 universal programmer. Current−voltage curves were recorded on an EG&G Princeton Applied Research model R-0151 *X*−*Y* recorder. A three-electrode system was used, consisting of a glassy carbon working electrode, a platinum counter electrode, and a saturated calomel reference electrode (SCE). UV−visible spectroelectrochemical experiments were carried out with a home-made thin-layer cell,[14] which has a light-transparent platinum gauze working electrode. The applied potential was monitored with an EG&G model 173 potentiostat, and UV−visible spectra were recorded on a Hewlett-Packard model 8453 diode array spectrophotometer.

Because the investigated $[Th_8TPyzPzM]$ complexes are highly aggregated in nonaqueous media, no meaningful electrochemistry and spectroelectrochemistry could be carried out on the neutral compounds without first "solubilizing" the material as described earlier for the case of "thiadiazolporphyrazines" [TTDPzM] [M = Zn^{II}, $Mg^{II}(H_2O)$, Cu^{II}, and $2H^{I}$].[2c] In the present paper, we first generated the triply reduced $[Th_8TPyzPzM]^{3-}$ derivatives, which were not aggregated in solution, and then examined the properties of the trianionic species as well as the singly and doubly reduced species in their monomeric forms. This was accomplished by first scanning to negative potentials to generate the more soluble trianion of each compound and then reversing the potential to 0.0 V to regenerate the neutral compound in its unaggregated form, after which the electrochemistry and UV−visible spectra could be measured. The electrogenerated monomers were moderately stable, and the UV−visible properties of each reduced form of the compounds could then be measured in a thin-layer cell in the absence of aggregation (see below).

Singlet Oxygen Quantum Yield Measurements. Measurements of the singlet oxygen quantum yield (Φ_Δ) of the complexes were carried out in DMF and in DMF added with aqueous HCl ([HCl] = 1×10^{-4} M; % V_{H_2O} = ca. 0.05%) by an absolute method reported in the literature[15a] and improved as reported elsewhere.[15b] 1,3-Diphenylisobenzofuran (DPBF) was used as the scavenger of $^1O_2$. Solutions of the complexes (ca. 10^{-6}−10^{-5} M) and DPBF (ca. 5×10^{-5} M) in DMF were irradiated in a 10-mm-path-length quartz cell with monochromatic light (Premier LC Lasers/HG Lens, Global Laser). The irradiation wavelength (λ_{irr} = 670 or 660 nm) was close to the maximum of the Q-band absorption peaks for all of the present octathienyl compounds and related octapyridino analogues (see Table 3). The light intensity was set to 0.300 mW and accurately measured with a radiometer (ILT 1400A/SEL100/F/QNDS2, International Light Technologies). The decay of DPBF absorption at 414 nm ($\varepsilon^{DPBF} = 2.3 \times 10^4$ mol^{-1} L cm^{-1}) was detected at 20 °C by a UV−visible spectrophotometer (Varian Cary 50 Scan).

The Φ_Δ values were obtained from the quantum yield of the photoreaction (Φ_{DPBF}) calculated with respect to different concentrations of DPBF, on the basis of eq 1,

$$\frac{1}{\Phi_{DPBF}} = \frac{1}{\Phi_\Delta} + \frac{k_d}{k_r}\frac{1}{\Phi_\Delta}\frac{1}{[DPBF]} \quad (1)$$

where k_d is the decay rate constant of $^1O_2$ in DMF and k_r is the rate constant of the reaction of DPBF with $^1O_2$. The $1/\Phi_\Delta$ value was

Table 1. UV−Visible Solution Spectra in Pyridine, DMSO, and DMF of the Thienyl Compounds $[Th_8TPyzPzM]\cdot xH_2O$ [M = $Mg^{II}(H_2O)$, Zn^{II}, Cu^{II}, Co^{II}, and $2H^{I}$] and Related Octapyridino Analogues $[Py_8TPyzPzM]$

compound	solvent	Soret region, λ [nm] (log ε)		Q-band region, λ [nm] (log ε)			ref
$[Th_8TPyzPzMg(H_2O)]\cdot 5H_2O$	py	387 (4.90)			609 (4.30)	674 (5.04)	tw
	DMSO	394 (4.90)			611 (4.50)	672 (4.90)	tw
	DMF	386 (4.90)			608 (4.30)	672 (5.04)	tw
$[Th_8TPyzPzZn]\cdot 4H_2O$	py	393 (5.10)			608 (4.60)	674 (5.40)	tw
	DMSO	390 (5.03)			609 (4.41)	672 (5.30)	tw
	DMF	395 (5.09)			609 (4.50)	672 (5.40)	tw
$[Th_8TPyzPzCu]\cdot 3H_2O$	py[a]	380				672	tw
$[Th_8TPyzPzCo]\cdot 2H_2O$	DMSO[b]	373	428 sh			656	tw
$[Th_8TPyzPz]^{2-}$	py[c]	391 (4.80)			614 (4.30)	679 (4.90)	tw
	DMSO[c]	393 (4.88)			614 (4.30)	679 (5.00)	tw
	DMF[c]	389 (4.90)			612 (4.30)	677 (5.00)	tw
$[Py_8TPyzPzMg(H_2O)]$	py	375 (5.23)		596 (4.65)	631 (4.64) sh	658 (5.54)	6b
	DMSO	374 (5.08)	566 (3.96) sh	594 (4.36)	629 (4.55) sh	653 (5.34)	6b
$[Py_8TPyzPzZn]$	py	378 (4.90)		598 (4.31)	630 (4.35) sh	658 (5.18)	6b
	DMSO	372 (5.10)	565 (4.54)	592 (4.54)	629 (4.61) sh	655 (5.36)	6b
$[Py_8TPyzPzCu]$	py	379 (4.64)		591 (4.18)		653 (4.93)	6b
	DMSO	365 (4.91)		590 (4.44)		648 (5.18)	6b
$[Py_8TPyzPzCo]$	py	364 (5.01)	441 (4.40)	575 (4.38) sh		635 (4.94)	6b
	DMSO	355 (5.23)	450 (4.65) sh	586 (4.71) sh		634 (5.24)	6b
$[Py_8TPyzPz]^{2-}$	py	362 (4.83)	402 sh	605 (4.39)	643 sh	667 (5.06)	4a
	DMSO	362	402 sh	607	635 sh	664	4a

[a] Qualitative spectrum obtained with a sample showing a low presence of aggregation. [b] Peak positions of the unreduced compound taken from the spectroelectrochemical data illustrated in Figure 6a. [c] ε values calculated referring to the neutral free-base $[Th_8TPyzPzH_2]\cdot CF_3COOH\cdot H_2O$.

obtained as the intercept of the Stern−Volmer plot ($1/\Phi_{DPBF}$ versus 1/[DPBF] (see Figure 8 in the Results and Discussion section), while the k_d/k_r value, which characterizes the decay of the $^1O_2$ scavenger in a certain solvent, is calculated by the ratio between the slope and intercept of each linear plot.

Fluorescence Measurements. Steady-state fluorescence and excitation spectra were obtained in DMF and acidified DMF (HCl) with a fluorescence spectrophotometer (Cary Eclipse, Varian) using a 10 mm quartz Suprasil cuvette. The fluorescence quantum yields were determined by a comparative method with a reference standard of chlorophyll *a* (Φ_F = 0.32, ether solution), according to eq 2, where *G* is the integrated emission area, *n* is the refractive index of the solvent, *A* is the absorbance at the excitation wavelength, and S and R indicate the sample and reference.

$$\Phi_F^S = \frac{G^S n_{DMF}^2 A^R}{G^R n_{ether}^2 A^S}\Phi_F^R \qquad (2)$$

In all cases, the absorbances of the solution were below 0.1 at and above the excitation wavelength.

Other Physical Measurements. IR spectra of the solid materials as KBr pellets were measured in the range of 4000−400 cm^{-1} with a Perkin-Elmer 1760 X spectrophotometer. UV−visible solution spectra other than those for spectroelectrochemistry (see above) were recorded with a Varian Cary 5E spectrometer. Elemental analyses for C, H, N, and S were provided by the "Servizio di Microanalisi" at the Dipartimento di Chimica, Università "La Sapienza" (Rome, Italy), on an EA 1110 CHNS-O instrument. Powder X-ray diffraction patterns were obtained on a Philips PW 1710 diffractometer by using Cu Kα (Ni-filtered) radiation.

RESULTS AND DISCUSSION

Preparation of Compounds and Solid-State Properties. The synthesis of the Mg^{II} complex was previously reported[12] and given the formula $[Th_8TPyzPzMg]$. The same formulation was used by the authors in a later report,[13] but in our hands, the investigated complex is assigned as the monohydrate $[Th_8TPyzPzMg(H_2O)]$. We have no direct evidence to prove the presence of a bound water molecule, but coordination of H_2O to magnesium(II) phthalocyanine and porphyrazine derivatives has often been demonstrated by single-crystal X-ray work, with two examples being the phthalocyanine complex $[PcMg(H_2O)]\cdot 2py$[16a] and the porphyrazine complex $[(omtp)Mg(H_2O)]$[16b] [omtp = octakis(methylthio)porphyrazinato dianion]. A dihydrate magnesium(II) phthalocyanine having the formula $[PcMg(H_2O)_2]$ has been isolated and its structure identified by X-ray work,[16c] as also a dimeric low-symmetry magnesium(II) porphyrazine monohydrate complex.[16d] Other magnesium(II) porphyrazines have been characterized by our group as monoaquo derivatives,[3a] including a magnesium(II) octapyridino analogue of the currently studied octathienyl derivative.[4b] As indicated in the Experimental Section, clathrated water is invariably observed in all of the currently synthesized octathienyl derivatives, the amount of which differed from batch to batch. The water of hydration is easily eliminated under mild conditions, but it again appears after exposure of the compounds to air. For the purpose of simplicity, the clathrated water is generally not shown in the formulas.

Solution UV−Visible Spectra. The examined octathienyl macrocycles are intense dark-blue/green amorphous materials that are completely insoluble in water and very poorly soluble in the nonaqueous nonpolar solvents CH_2Cl_2, $CHCl_3$, and low-polar benzonitrile, in which, based on UV−visible spectra (broad featureless absorptions of low intensity throughout the explored region), they manifest strong aggregation independent of the

dx.doi.org/10.1021/ic2007556 |*Inorg. Chem.* 2011, 50, 8225–8237

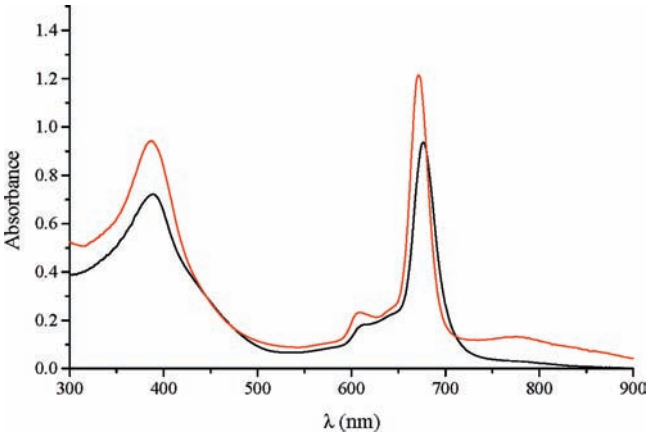

Figure 1. UV−visible solution spectra in DMF of $[Th_8PyzPzH_2]$ (black line) and $[Th_8PyzPzMg(H_2O)]$ (red line).

concentration. Better solubility is obtained in the polar solvents DMF, DMSO, and pyridine, in which, especially at the highest possible concentrations (ca. 10^{-4} M), aggregation is also present. This problematic aspect has been successfully overcome for the electrochemical studies, as described in the Experimental Section, and will be further illustrated below. Nevertheless, for many of the compounds, the monomeric form becomes largely prevalent at concentrations of ca. 10^{-5} M immediately after dissolution of the compounds or after some time so that, as specified in more detail below for each single species, quantitative UV−visible spectra and measurements of the quantum yields of singlet oxygen production were made possible.

The UV−visible spectral evolution of the Mg^{II} and Zn^{II} complexes in solutions of DMF, DMSO, and pyridine as a function of time systematically showed the complete formation of monomers. In these cases, the spectra of monomeric $[Th_8TPyzPzMg(H_2O)]$ and $[Th_8TPyzPzZn]$ display absorptions in the Soret (300−450 nm) and Q-band (600−700 nm) regions attributable to intraligand highest occupied molecular orbital (HOMO)−lowest unoccupied molecular orbital (LUMO) $\pi-\pi^*$ transitions, which is in line with the normally observed behavior for phthalocyanines and porphyrazines.[17] The UV−visible spectra of the Mg^{II} and Zn^{II} complexes are quite similar to each other in terms of the number of absorptions, their wavelength maxima, and the relative intensity of the bands (quantitative spectral data are given in Table 1). In addition, $[Th_8TPyzPzMg(H_2O)]$ in DMF often exhibited a broad peak of weak intensity in the lower-energy region of the spectrum, which can be attributed to aggregation. This band is seen at 700−900 nm in Figure 1 (red line) and disappeared upon heating of the solution to 70 °C for 30 min.

Unlike the Mg^{II} and Zn^{II} complexes, $[Th_8TPyzPzCu]$ and $[Th_8TPyzPzCo]$ remain aggregated in DMF and DMSO solutions after standing, and only qualitative spectra could be obtained (Table 1). In addition, $[Th_8TPyzPzCo]$, although it exhibits limited aggregation, tends to undergo a spontaneous one-electron reduction to its corresponding Co^{I} form, which has a UV−visible spectrum completely different from that of the neutral species (see further information on this point in the Electrochemical Measurements section).

As to the free-base macrocycle, the initially obtained UV−visible spectrum of $[Th_8TPyzPzH_2]$ in pyridine, DMSO, or DMF is characterized by a narrow unsplit Q band (Figure 1), indicative of the presence of the species in its deprotonated $[Th_8TPyzPz]^{2-}$

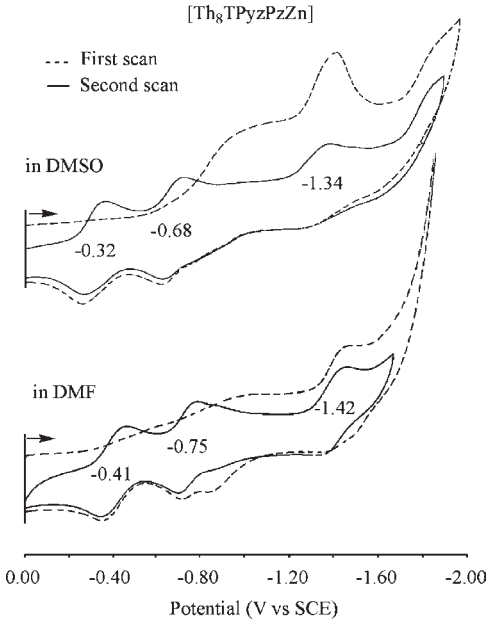

Figure 2. First (---) and second (—) scan of thin-layer cyclic voltammograms of $[Th_8TPyzPzZn]$ in DMSO and DMF (0.2 M TBAP).

dianionic form (D_{4h} symmetry). The octapyridinated analogue $[Py_8TPyzPzH_2]$ behaves differently in that in the same solvents it is initially aggregated. However, it shows a clean spectral evolution with the presence of isosbestic points that can be interpreted in terms of a dimer → monomer (dianionic) conversion.[4a]

From the spectral data in Table 1, it can be seen that peak maxima of the investigated compounds are practically independent of the solvent. The species $[Th_8TPyzPzM]$ [M = $Mg^{II}(H_2O)$, Zn^{II}, and Cu^{II}] and $[Th_8TPyzPz]^{2-}$ have Soret and Q bands that vary over a narrow range of 380−395 and 672−679 nm, respectively. The spectrum of the Co^{II} complex $[Th_8TPyzPzCo]$ is distinct from the other porphyrazines in that it exhibits Soret and Q bands whose peaks are shifted to lower wavelengths by an average of 15−20 and 25 nm, respectively. A comparison between UV−visible spectra of the octathienyl and octapyridinated compounds shows that the Soret and Q-band positions of the thienyl compounds are shifted *bathochromically* by about 20−25 nm for the metal complexes (the Co^{II} derivative included) and by 10−12 nm in the case of the free-base compound. These shifts are in the same direction as those observed for the octapyridino species upon quaternization of the external pyridine N atoms to give the cationic species $[(2\text{-Mepy})_8TPyzPzM]^{8+}$[6b] and $[(2\text{-Mepy})_8TPyzPz]^{6+}$.[6a] The resulting shifts in λ_{max} are also in the same direction as that upon formation of the homo- and heteropentametallic derivatives $[(PdCl_2)_4Py_8TPyzPzPd]$[5] and $[(PdCl_2)_4Py_8TPyzPzM]$,[7] where the average range of bathochromic shifts is 5−15 nm. These spectral shifts have been considered in direct relationship to the increased electron-withdrawing properties consequent to the charge location or coordination of $PdCl_2$ on the external pyridine rings. In light of these data, the parallel bathochromic spectral shifts observed for the thienyl compounds with respect to those observed for the series of the octapyridinated analogues can be taken as being directly related to the presence of the external thienyl rings, which evidently behave as strong electron-attracting fragments.

Electrochemical Measurements. Electrochemical and spectroelectrochemical measurements were carried out in pyridine,

dx.doi.org/10.1021/ic2007556 |*Inorg. Chem.* 2011, 50, 8225–8237

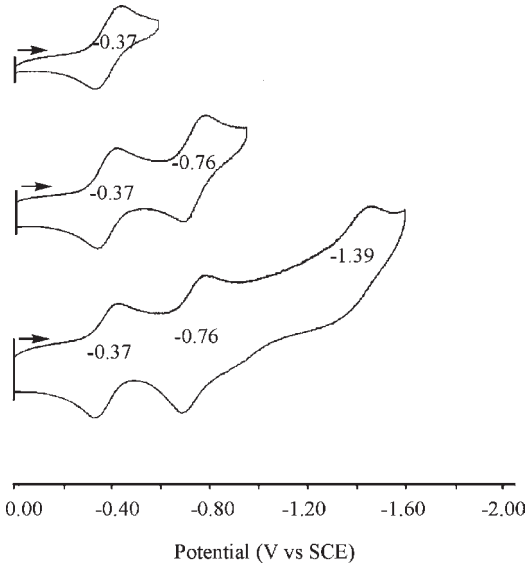

Figure 3. Second scan thin layer cyclic voltammograms of [Th_8TPyzPzZn] in pyridine (0.2 M TBAP).

DMSO, and DMF. Examples of thin-layer cyclic voltammograms are shown in Figures 2 and 3, which illustrate data for [Th_8TPyzPzZn] in DMSO, DMF, and pyridine. Aggregation, which dominates the UV−visible spectra at concentrations of ca. 10^{-5} M (see the earlier discussion), is even more evident at the concentrations used for electrochemical measurements ($\geq 10^{-4}$ M), and for this reason, a meaningful electrochemical response could not be obtained on the initial potential scan of the aggregated species (see the dashed line in Figure 2).

In contrast to the first negative potential scan from 0.00 to −2.00 V, useful electrochemical data were obtained in all cases on the second potential sweep (solid line in Figures 2 and 3). Under these experimental conditions, three of the four expected reductions are observed over the investigated potential range, the first of which occurs at $E_{1/2}$ = −0.32 to −0.41 V, the second at $E_{1/2}$ = −0.68 to −0.76 V, and the third at $E_{1/2}$ = −1.34 to −1.42 V, all vs SCE. Half-wave potentials of the Fc/Fc^+ couple were measured as 0.47, 0.50, and 0.53 V in DMSO, DMF, and pyridine, respectively, and the thermodynamic values of $E_{1/2}$ vs Fc/Fc^+ for the first reduction of [Th_8TPyzPzZn] are then given as −0.79 V (DMSO), −0.91 V (DMF), and −0.90 V (pyridine). These potentials are also listed in Table 2, which summarizes half-wave potentials for each metalated porphyrazine in the three solvents.

Several trends can be seen from the data in Table 2, the most evident of which is that the first reduction of the Co^{II} complex [Th_8TPyzPzCo] is substantially easier than that for reduction of the Zn^{II}, Mg^{II}, and Cu^{II} derivatives under the same solution conditions. At the same time, the second reduction of cobalt porphyrazine is harder (occurs at a more negative potential) than that of the other metalated compounds, thus leading to a much larger difference in $E_{1/2}$ (ΔE_{avg} = 650 mV) between the two processes as compared to the other three compounds, where an average $\Delta E_{1/2}$ = 340 mV is obtained in the three solvents. As described later in the manuscript, this difference in redox behavior is due to a different site of electron transfer for the Co^{II} complex and the other species.

There is also a marked solvent dependence of the measured $E_{1/2}$ values for all four compounds. The most facile first

Table 2. Half-Wave Potentials ($E_{1/2}$, V vs SCE and vs Fc/Fc^+) for the Reduction of [Th_8TPyzPzM] [M = Zn^{II}, $Mg^{II}(H_2O)$, Cu^{II}, and Co^{II}] in DMSO, DMF, and Pyridine (0.2 M TBAP)

		first reduction		second reduction		third reduction	
metal ion	solvent	vs SCE	vs Fc/Fc^+	vs SCE	vs Fc/Fc^+	vs SCE	vs Fc/Fc^+
Zn^{II}	DMSO	−0.32	−0.79	−0.68	−1.15	−1.34	−1.81
	DMF	−0.41	−0.91	−0.75	−1.25	−1.42	−1.92
	pyridine	−0.37	−0.90	−0.76	−1.29	−1.39	−1.92
$Mg^{II}(H_2O)$[a]	DMSO	−0.37	−0.84	−0.68	−1.15	−1.40	−1.87
	DMF	−0.43	−0.93	−0.77	−1.27	−1.41	−1.91
	pyridine	−0.46	−0.99	−0.79	−1.32	−1.49	−2.02
Cu^{II}	DMSO	−0.30	−0.77	−0.67	−1.14	−1.34	−1.81
	DMF	−0.26	−0.76	−0.60	−1.10	−1.24	−1.77
	pyridine	−0.35	−0.88	−0.67	−1.20	−1.36	−1.79
Co^{II}	DMSO[b]	−0.12	−0.59	−0.78	−1.25	−1.36	−1.83
	DMF	−0.13	−0.63	−0.82	−1.32	−1.36	−1.86
	pyridine	−0.25	−0.78	−0.85	−1.38	−1.35	−1.88

[a] Unknown impurity or side reaction seen for the Mg^{II} complex at $E_{1/2}$ = −0.98 to −1.04 V vs SCE in all solvents. [b] The oxidization of [Th_8TPyzPzCo^{II}] to [Th_8TPyzPzCo^{III}]$^+$ occurs at $E_{1/2}$ = 0.57 V in DMSO.

reduction occurs in DMSO for the M = Zn^{II}, Mg^{II}, and Co^{II} derivatives (see $E_{1/2}$ vs Fc/Fc^+ values listed in Table 2) but not for the Cu^{II} complex, where almost identical $E_{1/2}$ values of −0.77 and −0.76 V are obtained in DMSO and DMF. In contrast to the easier first reductions in DMSO, a more difficult first reduction is seen in pyridine for three of the four compounds (M = Mg^{II}, Cu^{II}, and Co^{II}) but not for zinc(II) porphyrazine, where virtually identical $E_{1/2}$ values of −0.90 and −0.91 V are measured in pyridine and DMF, respectively.

The second reduction of the Zn^{II} complex ranged from $E_{1/2}$ = −1.15 to −1.29 V vs Fc/Fc^+ in the three solvents, with a difference of 40 mV between the measured half-wave potentials in DMF and those in pyridine, with the easier reduction being in DMF. A 50 mV difference between $E_{1/2}$ in these two solvents is also seen for the Mg^{II} analogue, where an easier reduction again occurs in DMF. The same trend in ease of reduction is seen for the Cu^{II} complex in the same two solvents, but here a larger $\Delta E_{1/2}$ of 100 mV is observed between the two electron-transfer processes, which occur at $E_{1/2}$ = −1.10 and −1.20 V in DMF and pyridine, respectively (see Table 2). These differences in solvent effects on the redox potentials of the Zn^{II}, Mg^{II}, and Cu^{II} derivatives can be related to different interactions between the solvent and the three porphyrazines in their neutral, singly reduced, and doubly reduced forms.

Additional examples for thin-layer cyclic voltammograms of the four metalated compounds in pyridine, DMSO, and DMF are shown, in the order given, in Figures S2−S4, while voltammograms for the metalated compounds under "regular" cyclic voltammogram conditions are illustrated in Figures S5 (pyridine) and S6 (DMSO). The measured $E_{1/2}$ values are summarized in Table S1 and arranged according to solvent to better see how the potentials are shifted with changes in the metal ion under each solution condition. As earlier indicated, the half-wave potentials were recorded on the second potential sweep after the reductive breakup of the aggregates.

dx.doi.org/10.1021/ic2007556 |*Inorg. Chem.* 2011, 50, 8225–8237

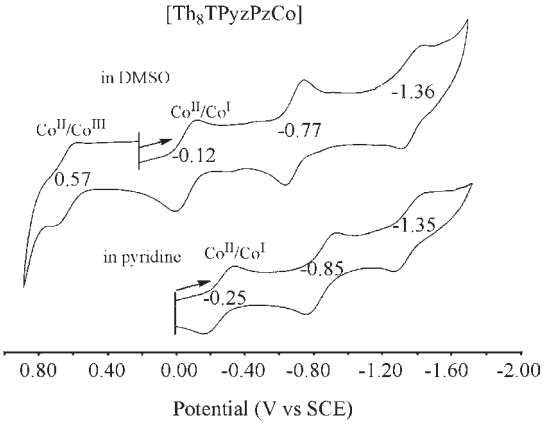

Figure 4. Thin-layer cyclic voltammograms of $[Th_8TPyzPzCo]$ in DMSO and pyridine (0.2 M TBAP).

No exchange of electrons is observed in the positive range of potentials for these compounds, with the exception of the Co^{II} complex, which undergoes three one-electron reductions and a single one-electron oxidation, which generates $[Th_8TPyzPzCo^{III}]^+$ in DMSO containing 0.1 M TBAP (see Figure 4, which illustrates cyclic voltammograms of the compound in DMSO and pyridine). The observation of a Co^{II}/Co^{III} process in DMSO but not in pyridine was also reported for $[Py_8TPyzPzCo]$[6b] and can be accounted for by a strong binding of one or two pyridine molecules to the Co^{II} form of the compound, which shifts $E_{1/2}$ for the metal-centered oxidation in pyridine to a value that is more positive of the solvent potential cutoff limit (about 0.7−0.8 V vs SCE). It should be pointed out that $[Py_8TPyzPzCo]$ undergoes a $Co^{II} \rightarrow Co^{I}$ process in DMSO, followed by a slow reverse process $Co^{I} \rightarrow Co^{II}$, and this reoxidation leads to isolation of the bis(DMSO) adduct $[Py_8TPyzPzCo(DMSO)_2]$, whose structure was elucidated by single-crystal X-ray work.[4c] In the same study,[4c] the Co^{I} and Co^{III} species, $Na[Py_8TPyzPzCo^{I}]$ and $[Py_8TPyzPzCo^{III}](SbCl_6)$, respectively, were isolated and characterized as solid materials via chemical pathways.

It should also be noted that current−voltage curves for the reduction and oxidation of $[Th_8TPyzPzCo]$ are much better defined than those for the other metalated compounds. This was true in all three solvents and can be accounted for by a lack of adsorption, which seems to be associated with the aggregated π-anion radical in the case of the Zn^{II}, Mg^{II}, and Cu^{II} derivatives. The degree of adsorption varies in strength as a function of the specific metal ion but is a maximum for M = Cu^{II} and a minimum for M = Zn^{II}, as can be seen in Figures S2−S4 in the Supporting Information. As described below, a cobalt(II) porphyrazine π-anion radical is not generated in first reduction of $[Th_8TPyzPzCo]$ but rather the first one-electron addition occurs at the metal center to give cobalt(I) porphyrazine with an unreduced π-ring system. The second reduction of $[Th_8TPyzPzCo]$ generates a cobalt(II) porphyrazine dianion as the final product, and thus no aggregation or adsorption is seen for cobalt porphyrazine in its π-anion radical form simply because this form of the compound does not exist on any appreciable time scale. This was also the case for the previously examined $[Py_8TPyzPzCo]$ (see Figure 4 in ref 6b).

As seen in Figures S2−S4 and Table S1 in the Supporting Information, the half-wave potential for the initial one-electron reduction of the $[Th_8TPyzPzM]$ compounds moves progressively toward more positive values in the order $Mg^{II} \rightarrow Zn^{II} \rightarrow Cu^{II} \rightarrow Co^{II}$, irrespective of the solvent used. The same order in ease of reduction is essentially maintained for the second, third, and fourth electron additions, with the exception of the Co^{II} complex, which has a different electron-transfer mechanism, as described below. The $E_{1/2}$ values in the "regular" and thin-layer cyclic voltammograms are almost identical for all of the examined porphyrazines, despite the different concentrations of supporting electrolyte used in each case (0.2 M TBAP in thin-layer experiments and 0.1 M in regular CV).

In summary, up to four stepwise one-electron reductions can be seen for each metalated porphyrazine in the three solvents. Because the Mg^{II}, Zn^{II}, and Cu^{II} metal ions are redox-inactive, the stepwise reductions must be considered as ring-centered and occur as shown by eqs 3−6.

$$[Th_8TPyzPzM] + e^- \rightleftarrows [Th_8TPyzPzM]^- \quad (3)$$

$$[Th_8TPyzPzM]^- + e^- \rightleftarrows [Th_8TPyzPzM]^{2-} \quad (4)$$

$$[Th_8TPyzPzM]^{2-} + e^- \rightleftarrows [Th_8TPyzPzM]^{3-} \quad (5)$$

$$[Th_8TPyzPzM]^{3-} + e^- \rightleftarrows [Th_8TPyzPzM]^{4-} \quad (6)$$

The proposed sequence of reduction steps for the Co^{II} complex is different from that of the other metalated derivatives in that the first one-electron addition occurs at the Co^{II} center to give cobalt(I) porphyrazine (eq 7), while the second one-electron reduction occurs at the macrocycle (eq 8a) and is followed by an internal electron transfer from the metal to the macrocycle (eq 8b) to give as a final product cobalt(II) porphyrazine with a doubly reduced macrocycle, i.e., $[Th_8TPyzPzCo^{II}]^{2-}$. The next two one-electron reductions of $[Th_8TPyzPzCo^{II}]^{2-}$ then proceed as shown in eqs 5 and 6.

$$[Th_8TPyzPzCo^{II}] + e^- \rightleftarrows [Th_8TPyzPzCo^{I}]^- \quad (7)$$

$$[Th_8TPyzPzCo^{I}]^- + e^- \rightleftarrows [Th_8TPyzPzCo^{I}]^{2-} \quad (8a)$$

$$[Th_8TPyzPzCo^{I}]^{2-} \rightarrow [Th_8TPyzPzCo^{II}]^{2-} \quad (8b)$$

An electrochemical reduction mechanism similar to that shown in eqs 7 and 8 was earlier proposed for the cobalt(II) octapyridino analogue $[Py_8TPyzPzCo]$[6b] as well as the diazepino compound $[Ph_8DzPzCo]$.[3b] Evidence for the sequence of steps given by eqs 7 and 8, followed by eqs 5 and 6 in the current study, is given, in part, by the similar spectrum of doubly reduced $[Th_8TPyzPzCo^{II}]^{2-}$ with the other three doubly reduced $[Th_8TPyzPzM]^{2-}$ compounds (see the Spectroelectrochemistry section) as well as by the fact that the third reduction potential of $[Th_8TPyzPzCo]^{2-}$ is quite close to $E_{1/2}$ values for the third reduction of $[Th_8TPyzPzM]^{2-}$, where M = Mg^{II} or Zn^{II}, independent of the solvent (see Tables 2 and S1).

The absolute potential separations between each stepwise reduction of the metalated complexes are also given in Table S1 and listed as Δ_{1-2}, Δ_{2-3}, and Δ_{3-4}. These separations vary little with changes in the central metal ion upon going from the porphyrazine with M = $Mg^{II}(H_2O)$ to Zn^{II} to Cu^{II} and the average $\Delta E_{1/2}$ values are 0.29, 0.63, and 0.32 V, respectively, in pyridine. Comparable average values of $\Delta E_{1/2}$ are seen for the same compounds in the other two solvents.

From the measured $E_{1/2}$ values in Tables 2 and S1 in the Supporting Information, it is clear that the stepwise addition of

dx.doi.org/10.1021/ic2007556 |Inorg. Chem. 2011, 50, 8225–8237

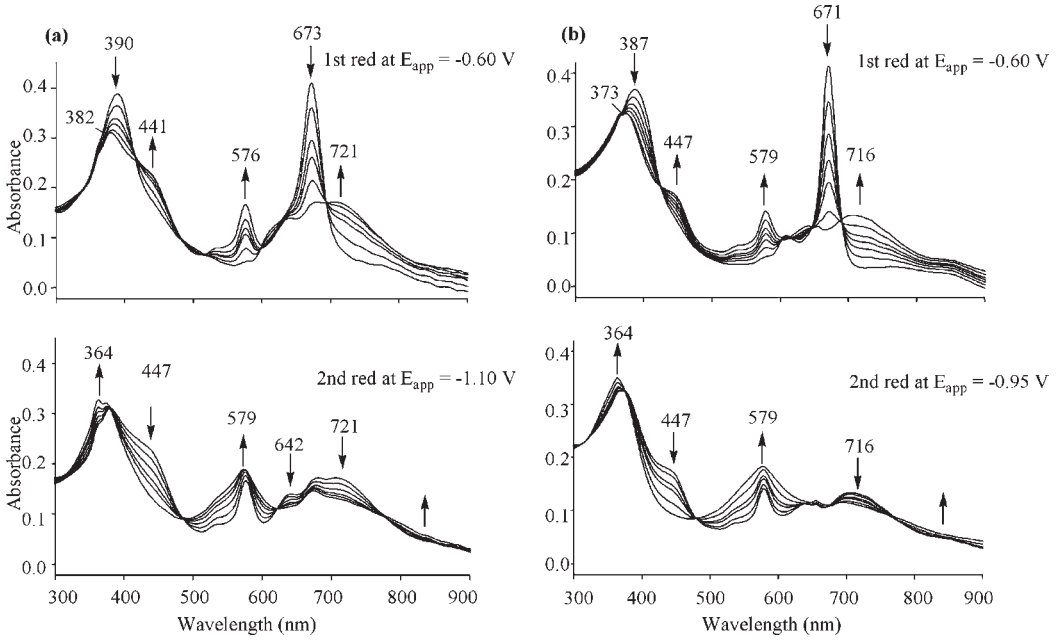

Figure 5. UV−visible spectral changes during first and second one-electron reductions of (a) [Th_8TPyzPzZn] and (b) [Th_8TPyzPzMg(H_2O)] in DMSO containing 0.2 M TBAP.

electrons to the series of [Th_8TPyzPzM] compounds takes place at much more positive $E_{1/2}$ values than those for the related phthalocyanine analogues,[18] a fact that is attributed to the presence of the strongly electron-withdrawing dithienylpyrazino fragments that replace the benzene rings of the phthalocyanine macrocycle (see Chart 1B). This shift in $E_{1/2}$ toward more positive potentials is a feature shared by the related diazepino-[3b] and thiadiazolporphyrazine[2c] macrocycles, with parallel results also being obtained for related compounds having peripheral dipyridinopyrazine fragments (Chart 1A)[4a,b,5] as well as for the octacationic[6b,5] (Figure S1A) and the homo-[5] and heteropentametallic[7] derivatives (Figure S1B).

Finally, it should be mentioned that the observed trend of reduction potentials as a function of solvent, metal ion, and structure approaches what was earlier reported for related electron-deficient macrocycles, each of which shares the feature of possessing a five-,[2] six-,[4−7] or seven-membered[3] heterocycle annulated to the four pyrrole rings of the porphyrazine core. A further common feature connecting these related compounds is that the electron deficiency of the macrocycle is associated with a facile redistribution and stabilization of the excess negative charge within the entire framework of the π-conjugated system.

Spectroelectrochemistry. UV−visible spectra for each reduced species were obtained by thin-layer spectroelectrochemistry, as described in the Experimental Section, and are discussed below in the order M = Mg^{II} and Zn^{II}, followed by Co^{II} and then $2H^1$. Although the cyclic voltammograms of the Cu^{II} complex enable $E_{1/2}$ values to be determined (see Figures S2−S6), aggregation and adsorption of the neutral and singly reduced complex were too extensive for obtaining meaningful measurements of UV−visible spectral changes after each stepwise one-electron reduction.

M = Mg^{II} and Zn^{II}. Figure 5 depicts the thin-layer UV−visible spectral changes that occur during the first two reductions of the Mg^{II} and Zn^{II} complexes in DMSO. An example of the thin-layer cyclic voltammogram for [Th_8TPyzPzZn] obtained under the same solution conditions as the thin-layer spectroelectrochemistry measurements is shown in Figure 2. Similar thin-layer voltammograms were obtained for [Th_8TPyzPzMg(H_2O)], whose half-wave potentials for reduction are listed in Table 2.

Each redox process of [Th_8TPyzPzZn] and [Th_8TPyzPzMg(H_2O)] is spectrally reversible, but as noted in the Experimental Section, it was necessary to first reduce the aggregated compounds to generate the trianion of the M^{II} species in its monomeric form. The applied potential was then set to 0.00 V to obtain the spectrum of the neutral compound in its monomeric form, after which the applied potential was shifted to more negative values, where the monomeric monoanion and dianion could be electrogenerated and their spectra recorded.

As seen in Figure 5, similar spectral changes occur during the first two reductions of monomeric [Th_8TPyzPzZn] and [Th_8TPyzPzMg(H_2O)] in DMSO. The multiple isosbestic points in the figures indicate the absence of any spectrally detectable intermediates in solution during the first two one-electron additions. A similarity in the spectra before and after electroreduction was earlier reported for the magnesium(II) and zinc(II) octapyridino analogues[6b] as well as for the tetrakis(thiadiazole)porphyrazine macrocycles [TTDPzM] [M = Mg^{II}(H_2O) and Zn^{II}][2c] having centrally the same two metal ions.

In the case of the zinc(II) and magnesium(II) thienylporphyrazines, there is a disappearance of the Q band at 671−673 nm, and the appearance of new absorption bands at ca. 576−579 and 716−721 nm as the monoanion is electrogenerated (see the top two spectra in Figure 5a,b). The 576−579 nm band further increases in intensity during the second reduction, while the 716−721 nm band decreases in intensity (see the lower two spectra in Figure 5a,b). An interpretation of these spectral features along with density functional theory (DFT) and time-dependent DFT (TDDFT) calculations has been published[2c] for the redox processes [TTDPzZn] → [TTDPzZn]$^-$ and [TTDPzZn]$^-$ → [TTDPzZn]$^{2-}$. The Zn^{II} complex was selected in the earlier theoretical study as

dx.doi.org/10.1021/ic2007556 |*Inorg. Chem.* 2011, 50, 8225–8237

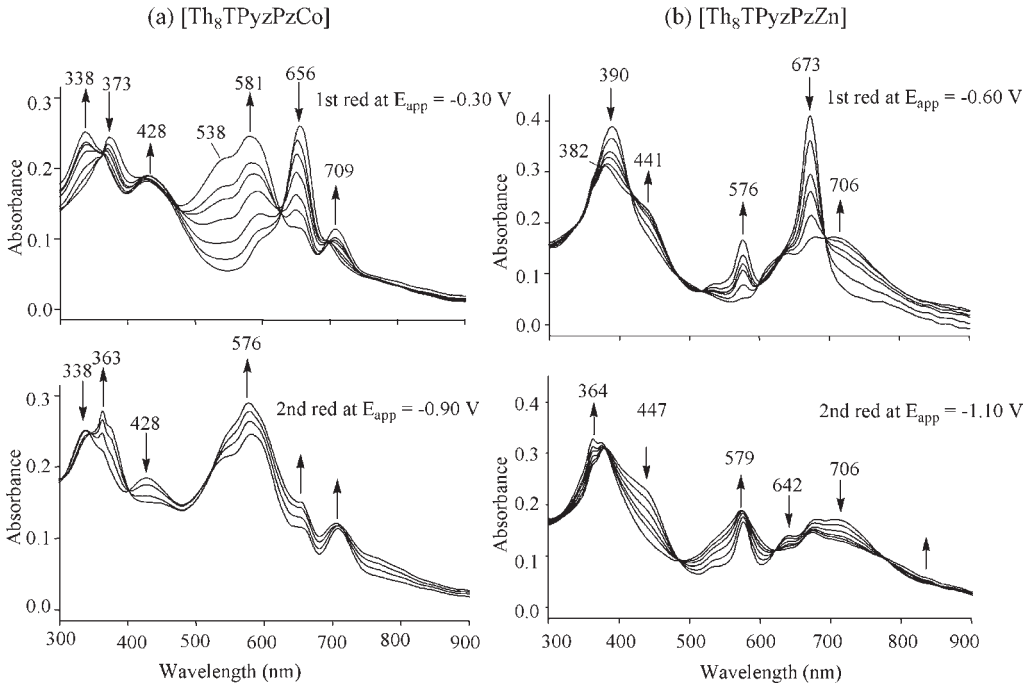

Figure 6. UV−visible spectral changes obtained during the first and second reductions of (a) [Th_8TPyzPzCo] and (b) [Th_8TPyzPzZn] in DMSO containing 0.2 M TBAP.

a representative compound describing the ground- and excited-state electronic structures of the entire series of neutral [TTDPzM][2b] and negatively charged $[TTDPzM]^{n-}$ derivatives [n = 1−4; M = Zn^{II}, $Mg^{II}(H_2O)$, Cu^{II}, and $2H^I$].[2c]

M = Co^II^. As indicated in eq 7, a metal-centered Co^{II}/Co^{I} process is assigned for the first reduction of [Th_8TPyzPzCo], which gives a stable Co^I complex. $[Th_8TPyzPzCo^I]^-$ is then further reduced in the second step to a transient $[Th_8TPyzPzCo^I]^{2-}$ species (eq 8a), which undergoes a rapid conversion of Co^I to Co^{II} to give as a final product the cobalt(II) porphyrazine dianion, $[Th_8TPyzPzCo^{II}]^{2-}$ (eq 8b).

The spectroelectrochemical data confirm the proposed mechanisms for the sequence of steps in the first two reductions (eqs 7 and 8). As seen in Figure 6a, the first reduction of [Th_8TPyzPzCo] leads to the spectrum of the 1− charged species, which exhibits an intense broad peak centered at 581 nm. At the same time, the initial Q band at 656 nm is red-shifted to 709 nm and decreases in intensity. The Soret band at 373 nm also decreases in intensity and shifts to 338 nm during this process. The final spectrum after the addition of one electron to give $[Th_8TPyzPzCo^I]^-$ is quite different from that of singly reduced $[Th_8TPyzPzZn^{II}]^-$ (Figure 6b) where a π-anion radical is generated, but the spectra obtained upon the second one-electron reduction of cobalt(II) and zinc(II) porphyrazines are quite similar to each other, with both dinegative species having bands at 576−579 and 363−364 nm (see the lower two spectra in Figure 6).

Similar spectral changes occur during the reduction of cobalt porphyrazine in pyridine as in DMSO, but in pyridine all three one-electron reductions of [Th_8TPyzPzCo] could be characterized in the thin-layer cell (Figure S7). The spectral evolutions in pyridine are similar to what was reported for the reduction of the octapyridino analogue.[6b] The broad peak at 581 nm for $[Th_8TPyzPzCo^I]^-$ can be considered as a metal-to-ligand charge-transfer band. A similar assignment was made for a broad peak in the spectra of the singly reduced phthalocyanine Co^{II} complex, [PcCo], in different solvents.[19−21]

In addition to three reversible reductions, the [Th_8TPyzPzCo] complex also undergoes a reversible one-electron oxidation at $E_{1/2}$ = 0.57 V in DMSO, a potential close to that measured for the Co^{II}/Co^{III} process of the octapyridino analogue in the same solvent (0.67 V).[6b] A comparison of the spectral changes for the two compounds is shown in Figure S8. The spectra of $[Th_8TPyzPzCo^{III}]^+$ and $[Py_8TPyzPzCo^{III}]^+$ are quite similar to each other in shape, with the main difference between the two being a bathochromic shift of Q bands for the neutral and singly oxidized compounds in the case of [Th_8TPyzPzCo].

M = 2H^I^. The free-base porphyrazine [Th_8TPyzPzH_2] undergoes five ill-defined reductions in pyridine, DMSO, and DMF, as seen in Figure 7. The third process at E_p = −1.02 to −1.07 V for a scan rate of 0.1 V s^{-1} is actually due to a reduction of dianionic $[Th_8TPyzPz]^{2-}$, which is in equilibrium with the neutral form of [Th_8TPyzPzH_2] as shown in eq 9:

$$[Th_8TPyzPzH_2] \rightleftarrows [Th_8TPyzPz]^{2-} + 2H^+ \quad (9)$$

In order to further investigate the equilibrium shown in eq 9, cyclic voltammograms were taken of [Th_8TPyzPzH_2] in pyridine containing 0.1 M TBAP and 0.12 M OH^- in the form of TBA(OH). Under these experimental conditions, the equilibrium in eq 9 is completely shifted to the right, and the first reduction occurs as shown in eq 10.

$$[Th_8TPyzPz]^{2-} + e^- \rightleftarrows [Th_8TPyzPz]^{3-} \quad (10)$$

The fact that two reductions at −0.23 and −0.47 V are no longer seen after adding TBA(OH) to the pyridine solvent containing [Th_8TPyzPzH_2] (Figure S9 in the Supporting Information) strengthens the conclusion that these processes are assigned as

dx.doi.org/10.1021/ic2007556 |*Inorg. Chem.* 2011, 50, 8225–8237

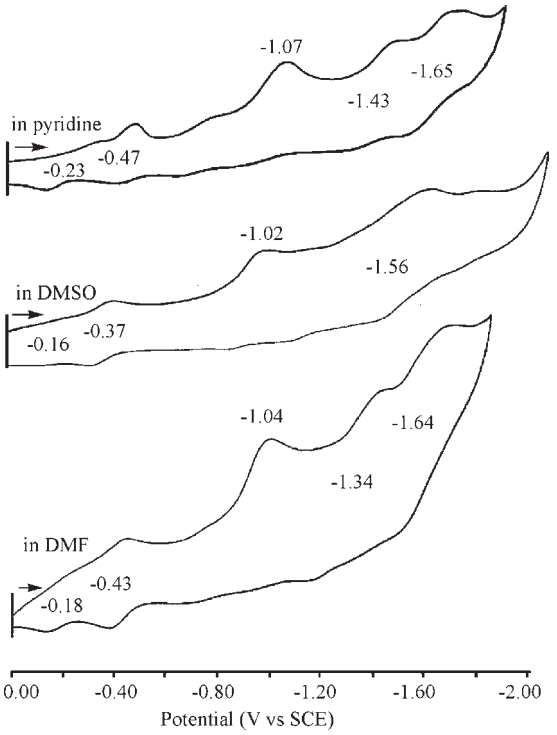

Figure 7. Cyclic voltammograms of $[Th_8TPyzPzH_2]$ in pyridine, DMSO, and DMF, all containing 0.1 M TBAP. Scan rate = 0.1 V s^{-1}.

the first and second reductions of the free-base neutral macrocycle $[Th_8TPyzPzH_2]$.

Figure S10 in the Supporting Information shows the UV−visible spectral changes that occur upon the first and second one-electron reductions of $[Th_8TPyzPzH_2]$ in pyridine, 0.1 M TBAP, to give $[Th_8TPyzPzH_2]^-$ in the first step and then $[Th_8TPyzPzH_2]^{2-}$ in the second. A similar series of reductions was earlier reported for $[Py_8TPyzPzH_2]$,[4a] and these reactions were not further examined as part of the current study.

Singlet Oxygen ($^1O_2$) and Fluorescence Quantum Yields. The use of porphyrins and phthalocyanines in photodynamic therapy (PDT) of cancer has been intensively studied.[8] In PDT, the efficiency of a tetrapyrrolic photosensitizer, measured by the quantum yield value of its singlet oxygen production (Φ_Δ), depends on the photophysical properties of its ground-to-excited-state pathway and, as a determinant factor, by the presence and type of a central metal ion. Usually, closed-shell central metal ions, like Zn^{II} and Mg^{II}, and in some cases, open-shell diamagnetic d^8 metal centers, like Pd^{II}, give rise to complexes with good photosensitizing capabilities. In this context, we recently demonstrated that Pd^{II}-pyridinated pyrazinoporphyrazines are photoactive in DMF solutions and act as singlet oxygen sensitizers.[22]

In the present study, Φ_Δ values were calculated from eq 1 using Stern−Volmer plots of the type shown in Figure 8 for the compound $[Th_8TPyzPzZn]$. The data obtained for the octathienylzinc(II) and -magnesium(II) and free-base porphyrazine compounds in DMF ($c \cong 10^{-5}$ M) and for the two metalated species in DMF acidified with HCl (DMF/HCl; $[HCl] = 1 \times 10^{-4}$ M) are listed in Table 3. Regardless of the presence or absence of HCl, the observed Φ_Δ values follow the order $Zn^{II} > Mg^{II}(H_2O) \cong$ free base. As can be seen in Table 3, the same order is mantained for the Zn^{II} and Mg^{II} octapyridinated analogues, $[Py_8TPyzPzZn]$ and $[Py_8TPyzPzMg(H_2O)]$[23] (Figure 1A), and their corresponding

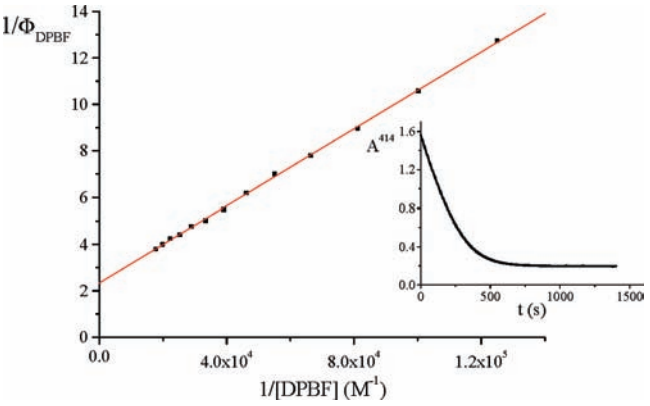

Figure 8. Stern−Volmer data analysis of the DPBF decay (see the inset) recorded during a Φ_Δ measurement of the complex $[Th_8TPyzPzZn]$ in DMF.

octacations $[(2\text{-Mepy})_8TPyzPzZn]^{8+}$ and $[(2\text{-Mepy})_8TPyzPzMg(H_2O)]^{8+}$ (Figure S1A).

Higher Φ_Δ values for the Zn^{II} species as compared to those of the Mg^{II} compounds are in line with expectation, in view of the heavy atom effect, which favors Zn^{II}. The Φ_Δ values of the Zn^{II} species (0.4−0.6) are in the range 0.4−0.7 observed for a number of zinc(II) porphyrazines,[9−11] and this qualifies them as excellent photosensitizers for the generation of singlet oxygen. It should be pointed out that the photoactive *water-soluble* Zn^{II} octacation $[(2\text{-Mepy})_8TPyzPzZn]^{8+}$ was very recently shown[25] to form complexes with a G-quadruplex (G4) DNA structure of the telomeric sequence 5′-d[AGGG(TTAGGG)$_3$]-3′ in aqueous media containing K^+. These results are strictly connected with studies in which guanine reach sequences have become important for the development of new antitumoral drugs, and this then qualifies the Zn^{II} octacation as a potential bimodal anticancer agent.

It can be noticed from the data in Table 3 that, for the octathienylzinc(II) and -magnesium(II) compounds, the Φ_Δ values increase upon going from DMF to DMF/HCl. This trend is also followed for the octapyridino analogues and their corresponding octacations. The increase of the Φ_Δ values for the Zn^{II} macrocycles is in the narrow range of 0.03−0.10, whereas the change for the Mg^{II} compounds is remarkably higher (0.13−0.26) and comparable to the absolute Φ_Δ values normally obtained for the magnesium(II) porphyrazine sensitizers. In our previous work on octapyridinated palladium(II) porphyrazines, the use of DMF acidified with HCl (molar ratio macrocycle/HCl of 1:10)[22] was shown to be necessary to successfully overcome the tendency of these species to undergo a one-electron reduction in DMF. This reduction process is ascribed to small amounts of reducing agents (dimethylammine?) normally present in the solvent at a level of concentration comparable with that of the macrocycles, and it was shown that HCl is able to reoxidize the reduced forms or to avoid reduction with preacidification.

Among the compounds listed in Table 3, there are no cases for which preacidification with HCl (1×10^{-4} M) was strictly required because no tendency to reduction was, in general, observed in DMF with the exception of the Zn^{II}-pyridinated octacation $[(2\text{-Mepy})_8TPyzPzZn]^{8+}$. This species, at a concentration of about 10^{-5} M, occasionally (depending on the stock of solvent) shows a tendency to undergo a one-electron reduction, a process that systematically occurs at lower concentrations

dx.doi.org/10.1021/ic2007556 |*Inorg. Chem.* 2011, 50, 8225–8237

Table 3. Singlet Oxygen (Φ_Δ) and Fluorescence (Φ_F) Quantum Yields in DMF

compound	[HCl] (M)	λ_{max} (Q band) (nm)	λ_{irr} [a] (nm)	Φ_Δ [b]	$k_d/k_a \times 10^5$ [c,d] (M)	λ_{em} ($\Delta\lambda$) [e] (nm)	Φ_F [b]	ref
[Th_8TPyzPzZn]	0	672	670	0.43[f]	3.5	679(8)	0.15[g]	tw
	1×10^{-4}	672	670	0.51	3.1	680(8)	0.17[g]	tw
[Th_8TPyzPzMg(H_2O)]	0	672	670	0.14	3.1	679(7)	0.11[g]	tw
	1×10^{-4}	669	670	0.27	3.1	677(8)	0.40[g]	tw
[Th_8TPyzPz]$^{2-}$	0	677	670	0.19	3.2	681(4)	0.09[g]	tw
[Py_8TPyzPzZn]	0	657	660	0.55	3.5	664(7)	0.23[h]	23
	1×10^{-4}	657	660	0.58	2.8	664(7)	0.17[h]	23
[Py_8TPyzPzMg(H_2O)]	0	658	660	0.09	2.9	665(7)	0.10[h]	23
	1×10^{-4}	653	660	0.29	3.0	663(10)	0.43[h]	23
[(2-Mepy)$_8$TPyzPzZn]$^{8+}$	0	666	660	0.29	2.8			
	1×10^{-4}	666	660	0.40	2.8	673(7)	0.17[h]	tw
[(2-Mepy)$_8$TPyzPzMg(H_2O)]$^{8+}$	0	669	660	~0	2.8	678(9)	~0[g]	tw
	1×10^{-4}	664	660	0.26	2.8	672(8)	0.36[g]	tw

[a] Wavelength of laser source irradiation. [b] Mean value of at least three measurements. The uncertainty is half-dispersion, and it is typically ±0.03. [c] The list of reported values, which depend exclusively on the scavenger and the solvent used, is close to the previously published data for similar measurements: $(2.9 \pm 0.3) \times 10^{-5}$ M (DMF),[15] $(3.7 \pm 0.4) \times 10^{-5}$ M (DMF),[24] and $(3.0 \pm 0.2) \times 10^{-5}$ M (DMF/HCl).[24] [d] Uncertainty: ±0.1. [e] $\Delta\lambda$ is the Stokes shift, which moves in the range 4−10 nm. [f] The value measured in pyridine for this compound was 0.635.[13] [g] Excitation wavelength: 620 nm. [h] Excitation wavelength: 600 nm.

($c \leq 10^{-6}$ M; see below). Because no tendency to reduction is seen for the octathienylzinc(II) and -magnesium(II) compounds, the increment of Φ_Δ observed in the presence of HCl might be attributed to the elimination of residual forms of aggregation, which are not observed by UV−visible and spectroelectrochemical studies of the compounds. Disaggregation might go through the interaction of the H atom of polarized $H^{\delta+}Cl^{\delta-}$ with the basic centers (N and S atoms) of the octathienyl macrocycle or even by the attraction of the Cl atom with the metal center. Although the relatively small increase of Φ_Δ for the Zn^{II} species might be explained in such a way, it appears difficult to justify the observed variations for the Mg^{II} compounds on the same basis.

Fluorescence quantum yields (Φ_F) and Stokes shifts ($\Delta\lambda$) obtained in DMF and DMF/HCl for the Zn^{II} and Mg^{II} species ($\leq 10^{-6}$ M) are also listed in Table 3. Small Stokes shifts (4−10 nm) are observed for all in the compound series, as is normally found for porphyrazine macrocycles. Figure 9 shows, as a representative example, the absorption, excitation, and emission spectra of the Zn^{II} complex [Th_8TPyzPzZn]. The overall coincidence of the narrow Q band as to the absorption and excitation spectra, common to all of the compounds, indicates that monomeric species are almost exclusively present in solution.

Among the Φ_F values reported in Table 3, the value of the Zn^{II} octacation [(2-Mepy)$_8$TPyzPzZn]$^{8+}$ in DMF in the absence of HCl could not be obtained because at the low concentration used for the measurements the complex undergoes a one-electron reduction. The Φ_F values of the Zn^{II} species in DMF or DMF/HCl are lower than the corresponding Φ_Δ values, which is in line with expectation. The small changes of the Φ_F values for the Zn^{II} species determined by acidification are in striking contrast with the parallel changes of the Mg^{II} species. For these latter ones, Φ_F variations are 0.11 (DMF) → 0.40 (DMF/HCl) and 0.10 (DMF) → 0.43 (DMF/HCl) for the octathienyl and octapyridino compounds, respectively, and ~0 (DMF) → 0.36 (DMF/HCl) for the octacationic species (Table 3). In light of these data, the hypothesis that the observed changes might be due to disaggregation phenomena appears inadequate. The observed behavior suggests that more advanced studies are needed, especially in light of the fluorescence values (0.36−0.43) in DMF/HCl, which appear to be of interest in the area of medical imaging response and diagnosis.

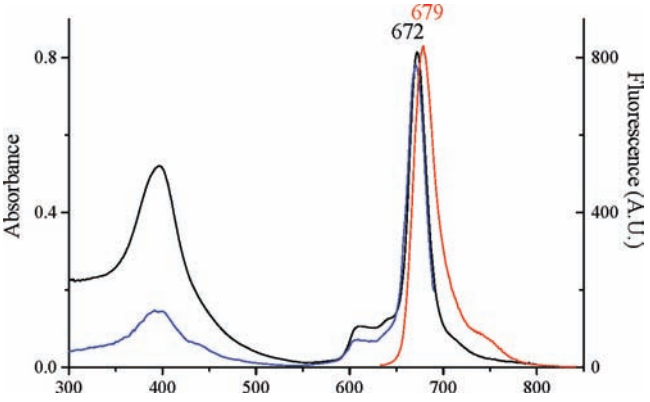

Figure 9. UV−visible absorption (black line), excitation (blue line; λ_{em} = 690 nm), and emission (red line; λ_{exc}= 620 nm) spectra of the complex [Th_8TPyzPzZn] in DMF.

CONCLUSIONS

UV−visible spectral solution studies carried out in DMF, DMSO, and pyridine on a series of octathienyl pyrazinoporphyrazine macrocycles having the formula [Th_8TPyzPzM] [M = Mg^{II}(H_2O), Zn^{II}, Co^{II}, Cu^{II}, and $2H^1$; Chart 1B] indicate that all of the compounds behave as highly electron-deficient macrocycles because of the presence of the external electron-withdrawing 2-thienyl rings. Cyclic voltammetry and spectroelectrochemical measurements show generally clean reversible or quasi-reversible stepwise one-electron reductions, leading to the formation of 1−, 2−, 3−, and 4− charged species at half-wave potential values markedly less negative than those of the parent phthalocyanine compounds, the behavior approaching that of the

dx.doi.org/10.1021/ic2007556 |Inorg. Chem. 2011, 50, 8225–8237

parallel series of octapyridinated analogues. The uptake of electrons by these compounds induces spectral changes that also closely resemble those of the parent octapyridinated species. The Co^{II} complex deserves special mention because of its distinct behavior in the first and second one-electron reductions both metal-centered, implying the sequence $Co^{II} \rightarrow Co^{I}$ followed by the reverse process $Co^{I} \rightarrow Co^{II}$ with formation of the species $[Th_8TPyzPzCo^{I}]^-$ and $[Th_8TPyzPzCo^{II}]^{2-}$, respectively. Moreover, the Co^{II} complex is the only one among the examined porphyrazines that undergoes one-electron oxidation in the range of potentials explored (0.00 to 1.6 V vs SCE), leading to formation of the species $[Th_8TPyzPzCo^{III}]^+$. The octathienylzinc(II) compound and its parent octapyridinated neutral and octacationic species are active photosensitizers for the generation of singlet oxygen in solutions of DMF and DMF/HCl (Φ_Δ = 0.4−0.6). Fluorescence measurements on the compounds indicate high Φ_F values for the parent Mg^{II} species (0.36−0.43) in DMF/HCl. Both types of data (Φ_Δ, Zn^{II}; Φ_F, Mg^{II}) open perspectives for their use in PDT of cancer and for medical imaging and diagnosis.

■ ASSOCIATED CONTENT

Supporting Information. Table S1 (cyclic voltammetric data), Figure S1 (schematic representations of macrocycles), Figures S2−S6 and S9 (cyclic voltammograms), and Figures S7, S8, and S10 (UV−visible spectral changes). This material is available free of charge via the Internet at http://pubs.acs.org.

■ AUTHOR INFORMATION

Corresponding Author

*E-mail: mariapia.donzello@uniroma1.it (M.P.D.), kkadish@uh.edu (K.M.K.).

■ ACKNOWLEDGMENT

M.P.D. acknowledges financial help from the Università "La Sapienza" (Ateneo, 2010) and the MIUR (Ministero dell'Università e della Ricerca Scientifica; PRIN 2007XWBRR4). The support of the Robert A. Welch Foundation (to K.M.K., Grant E-680) is gratefully acknowledged. G.D.M. thanks the Consorzio Interuniversitario di Ricerca in Chimica dei Metalli nei Sistemi Biologici (CIRCMSB) for an annual grant (2010).

■ REFERENCES

(1) (a) Stuzhin, P. A.; Ercolani, C. In *The Porphyrin Handbook*; Kadish, K. M., Smith, K. M., Guilard, R., Eds.; Academic Press: New York, 2003; Vol. 15, Chapter 101, pp 263−364. (b) Kudrevich, S. V.; van Lier, J. E. *Coord. Chem. Rev.* **1996**, *156*, 163–182. (c) Michel, S. L. J.; Hoffman, B. M.; Baum, S. M., Barrett, A. G. M. *Progress in Inorganic Chemistry*; Karlin, K. D., Ed.; John Wiley & Sons: New York, 2001; Vol. 50, pp 473−591.

(2) (a) Donzello, M. P.; Ercolani, C.; Stuzhin, P. A. *Coord. Chem. Rev.* **2006**, *250*, 1530–1561 and references cited therein. (b) Donzello, M. P.; Ercolani, C.; Kadish, K. M.; Ricciardi, G.; Rosa, A.; Stuzhin, P. A. *Inorg. Chem.* **2007**, *46*, 4145. (c) Donzello, M. P.; Ercolani, C.; Kadish, K. M.; Ricciardi, G.; Rosa, A. *Inorg. Chem.* **2009**, *48*, 9890. (d) Donzello, M. P.; Fujimori, M.; Yoshikawa, H.; Awaga, K.; Ercolani, C. *J. Porphyrins Phthalocyanines* **2010**, *14*, 343.

(3) (a) Donzello, M. P.; Ercolani, C.; Stuzhin, P. A.; Chiesi-Villa, A.; Rizzoli, C. *Eur. J. Inorg. Chem.* **1999**, 2075. (b) Donzello, M. P.; Dini, D.; D'Arcangelo, G.; Zhan, R.; Ou, Z.; Ercolani, C.; Stuzhin, P. A.; Kadish, K. M. *J. Am. Chem. Soc.* **2003**, *125*, 14190. (c) Donzello, M. P.; Ercolani, C.; Mannina, L.; Viola, E.; Bubnova, A.; Khelevina, O. G.; Stuzhin, P. A. *Aust. J. Chem.* **2008**, *61*, 262.

(4) (a) Donzello, M. P.; Ou, Z.; Meneghetti, M.; Ercolani, C.; Kadish, K. M. *Inorg. Chem.* **2004**, *43*, 8626. (b) Donzello, M. P.; Ou, Z.; Dini, D.; Meneghetti, M.; Ercolani, C.; Kadish, K. M. *Inorg. Chem.* **2004**, *43*, 8637. (c) Viola, E.; Donzello, M. P.; Ciattini, S.; Portalone, G.; Ercolani, C. *Eur. J. Inorg. Chem.* **2009**, 1600.

(5) Donzello, M. P.; Viola, E.; Cai, X.; Mannina, L.; Rizzoli, C.; Ricciardi, G.; Ercolani, C.; Kadish, K. M.; Rosa, A. *Inorg. Chem.* **2008**, *47*, 3903.

(6) (a) Bergami, C.; Donzello, M. P.; Ercolani, C.; Monacelli, F.; Rizzoli, C. *Inorg. Chem.* **2005**, *44*, 9852. (b) Bergami, C.; Donzello, M. P.; Monacelli, F.; Ercolani, C.; Kadish, K. M. *Inorg. Chem.* **2005**, *44*, 9862.

(7) Donzello, M. P.; Viola, E.; Cai, X.; Mannina, L.; Ercolani, C.; Kadish, K. M. *Inorg. Chem.* **2010**, *49*, 2447.

(8) (a) Moreira, L. M.; Vieira dos Santos, F.; Pereira Lyon, J.; Maftoum-Costa, M.; Pacheco-Soares, C.; Soares da Silva, N. *Aust. J. Chem.* **2008**, *61*, 741. (b) O'Connor, A. E.; Gallagher, W. M.; Byrne, A. T. *Photochem. Photobiol.* **2009**, *85*, 1053. (c) Szacilowski, K.; Macyk, W.; Drzewiecka-Matuszek, A.; Brindell, M.; Stochel, G. *Chem. Rev.* **2005**, *105*, 2647–2694. (d) Detty, M. R.; Gibson, S. L.; Wagner, S. J. *J. Med. Chem.* **2004**, *47*, 3897. (e) De Rosa, M. C.; Crutchley, R. J. *Coord. Chem. Rev.* **2002**, *233*−*234*, 351–371. (f) Pandey, R. K.; Zheng, G. In *The Porphyrin Handbook*; Kadish, K. M., Smith, K. M., Guilard, R. Eds.; Academic Press: New York, 2000; Vol. 6, Chapter 43, pp 157−230.

(9) (a) Zimcik, P.; Novakova, V.; Miletin, M.; Kopecky, K. *Macroheterocycles* **2008**, *1*, 21 and references cited therein. (b) Mitzel, F.; Fitzgerald, S.; Beeby, A.; Faust, R. *Eur. J. Org. Chem.* **2004**, 1136.

(10) (a) Baum, S. M.; Trabanco, A. A.; Montalban, A. G.; Micallef, A. S.; Zhong, C.; Meunier, H. G.; Suhling, K.; Phillips, D.; White, A. J. P.; Williams, D. J.; Barrett, A. G. M.; Hoffman, B. M. *J. Org. Chem.* **2003**, *68*, 1665. (b) Sakellariou, E. G.; Montalban, A. G.; Meunier, H.; Rumbles, G.; Philips, D.; Ostier, R. B.; Suhling, K.; Barrett, A. G. M.; Hoffman, B. M. *Inorg. Chem.* **2002**, *41*, 2182. (c) Montalban, A. G.; Baum, S. M.; Barrett, A. G. M.; Hoffman, B. M. *Dalton Trans.* **2003**, 2093.

(11) Michelsen, U.; Kliesch, H.; Schnurpfeil, G.; Sobbi, A. K.; Wöhrle, D. *Photochem. Photobiol.* **1996**, *64*, 694.

(12) Mørkved, E. H.; Ossleten, H.; Kjøsen, H.; Bjørlo, O. *J. Prakt. Chem.* **2000**, *342*, 83.

(13) Mørkved, E. H.; Afseth, N. Kr.; Zimcik, P. *J. Porphyrins Phthalocyanines* **2007**, *11*, 130.

(14) Lin, X. Q.; Kadish, K. M. *Anal. Chem.* **1985**, *57*, 1849.

(15) (a) Spiller, W.; Kliesch, H.; Wöhrle, D.; Hackbarth, S.; Röder, B.; Schnurpfeil, G. *J. Porphyrins Phthalocyanines* **1998**, *2*, 145. (b) Viola, E.; Donzello, M. P.; Giustini, M.; Monacelli, F.; Ercolani, C., to be submitted.

(16) (a) Fisher, M. S.; Templeton, D. H.; Zalkin, A.; Calvin, M. *J. Am. Chem. Soc.* **1971**, *93*, 2622. (b) Velasquez, S. V.; Fox, G. A.; Broderick, W. E.; Andersen, K. A.; Anderson, O. P.; Barrett, A. G. M.; Hoffman, B. M. *J. Am. Chem. Soc.* **1992**, *114*, 7416. (c) Matzumoto, S.; Endo, A.; Mizuguchi, J. *Z. Krystallogr.* **2000**, *215*, 182. (d) Baum, S. M.; Trabanco, A. A.; Montalban, A. G.; Micallef, A. S.; Zhong, C.; Meunier, H. G.; Suhling, K.; Phillips, D.; White, A. J. P.; Williams, D. J.; Barrett, A. G. M.; Hoffman, B. M. *J. Org. Chem.* **2003**, *68*, 1665.

(17) (a) Stillman, M. J. In *Phthalocyanines: Properties and Applications*; Leznoff, C. C., Lever, A. B. P., Eds.; VCH Publishers, Inc.: New York, 1989; Vol. 1, pp 133−289. (b) Mack, J.; Stillman, M. J. In *The Porphyrin Handbook*; Kadish, K. M., Smith, K. M., Guilard, R., Eds.; Academic Press: New York, 2003; Vol. 16, pp 43−116. (c) Gouterman, M. In *The Porphyrins*; Dolphin, D., Ed.; Academic Press: New York, 1978; Vol. III, and references cited therein.

(18) Clack, D. W.; Hush, N. S.; Woolsey, I. S. *Inorg. Chim. Acta* **1976**, *19*, 129.

(19) Stillman, M. J.; Thomson, A. J. *J. Chem. Soc., Faraday Trans. 2* **1974**, *70*, 790.

(20) Day, P.; Hill, H. A. O.; Price, M. *J. Chem. Soc. A* **1968**, 90.

(21) Clack, D. W.; Hush, N. S.; Yandle, J. R. *Inorg. Chem.* **1972**, *11*, 1738.

(22) Donzello, M. P.; Viola, E.; Bergami, C.; Dini, D.; Ercolani, C.; Giustini, M.; Kadish, K.; Meneghetti, M.; Monacelli, F.; Rosa, A.; Ricciardi, G. *Inorg. Chem.* **2008**, *47*, 8757. See also note *c* of Table 4 in ref 23.

(23) Donzello, M. P.; Vittori, D.; Viola, E.; Manet, I.; Mannina, L.; Monti, S.; Ercolani, C., C. *Inorg. Chem.* **2011**, DOI: 10.1021/ic200498s.

(24) Zimcik, P.; Miletin, M.; Musil, Z.; Kopecky, K.; Kubza, L.; Brault, D. *J. Photochem. Photobiol., A* **2006**, *183*, 59.

(25) Manet, I.; Manoli, F.; Donzello, M. P.; Viola, E.; Andreano, G.; Masi, A.; Cellai, L.; Monti, S. *Org. Biol. Chem.* **2011**, *9*, 684.